Computer-Aided Neuroanatomy: Differential Geometry of Cortical Surfaces and an Optimal Flattening Algorithm

Eric L. Schwartz
New York University Medical Center, NSK Institute,
and Courant Institute of Mathematical Sciences

Bjorn Merker
New York University Medical Center

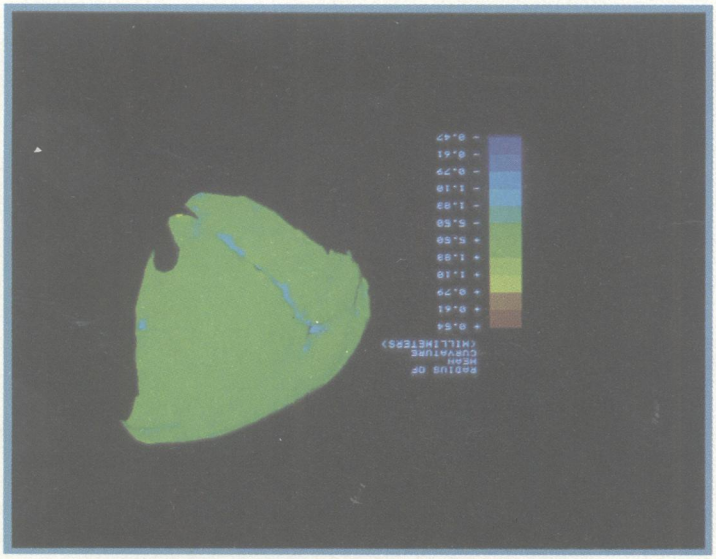

In a variety of species including monkeys and humans, the surface of the retina is mapped in an accurate manner to the surface of primary visual cortex. In a real sense there is an image, expressed in the firing density of neurons, impressed on the surface of the brain. The various images found in the brain have complicated natures: They are "distorted" by nonlinear map functions, and contain submodality information expressed spatially in the form of columnar systems representing stereo, orientation, motion, and other forms of data. The detailed study of such maps represents a difficult series of problems in the areas of computer graphics, image processing, numerical analysis, and neuroanatomy.

This article describes some initial steps in the field of computer-aided neuroanatomy. An algorithm for unfolding and flattening cortical surfaces and a measurement of the differential geometric aspects of these surfaces are presented. Models of the structure of images as they would appear mapped to the surface of primate striate cortex are also shown.

In this article we review several computer graphics and image processing applications that help us understand the architecture of monkey and human visual cortex. Two general areas are covered. First, computer graphics methods can be used to simulate the patterns of activity that would occur at various levels of the nervous system as a result of the presence of a particular image on the retina. Current understanding of brain architecture is sufficiently advanced to make this a useful exercise. Simulations of several aspects of visual cortex architecture, using real images, are presented.

Second, the technical aspects of studying brain architecture involve the reconstruction of patterns of architecture from serial sections. Computer graphics and image processing techniques can make a major contribution to this area by providing methods of reconstructing the three-dimensional surfaces derived from large numbers of serial sections, and also by providing flattened versions of these surfaces. We have termed this area of application *computer-aided anatomy*.[1]

We illustrate this methodology by demonstrating an algorithm we have developed that flattens a 3D reconstruction of the opercular surface of monkey striate cortex while optimally preserving the metric structure of the original neural surface. As a first step in this work, we have measured the mean and Gaussian curvature[2] at each point of the opercular surface of macaque striate cortex. We thus demonstrate a complete characterization of the differential geometric structure of a cortical surface, as well as a means of optimally flattening this surface for purposes of measurement and display.

Primate visual cortex

First we present a very brief review of the terminology and some of the phenomenology of primate visual cortex. The term *cortex*, derived from Latin, refers to "skin" or "bark." Many structures in the central nervous system are cortical in architecture: They are essentially two-dimensional sheets in which the surface area is on the order of 100 to 1000 mm,[2] while the thickness is on the order of 1 mm. Furthermore, much recent work in this field has demonstrated remarkable fine structure within single layers of individual cortical areas. These observations have been grouped together under the term *functional architecture*.[3] Three examples follow:

0272-1716/86/0300-0036$01.00 © 1986 IEEE

1. In the topographic structure of striate (V1) cortex there is a point-to-point correspondence between the retinal surface and the input layers of primary visual cortex. Figure 1 shows an example of a mathematical model of this mapping, as well as several recent experimental measurements. Three recent, independent experiments have found that the theoretical map function[4] used in Figure 1 is a good approximation to the current understanding of this data.[5–8]

2. There are ocular dominance columns in striate cortex: The left and right eyes terminate, in the input layers of striate cortex of man and monkey, in a zebra-striped pattern, also shown in Figure 1. Each individual stripe (left or right eye input) is called an ocular dominance column.[3] This interlacing of left and right eye input, on the scale of 0.5 mm, may be related to stereo vision.

3. Orientation columns, as described by Hubel, Wiesel, and Livingstone,[3,9] are thin (50 micron × 500 micron) slabs of tissue consisting of cells that respond to oriented "edges" of roughly the same orientation in the visual field.

Features 2 and 3 above suggest that a small patch of cortical tissue, on the order of 1 mm in size, contains a complete left-right eye representation as well as a complete set of orientation columns spanning a full 180 degrees. Hubel and Wiesel[3] coined the term hypercolumn to refer to a such a complete processing module.

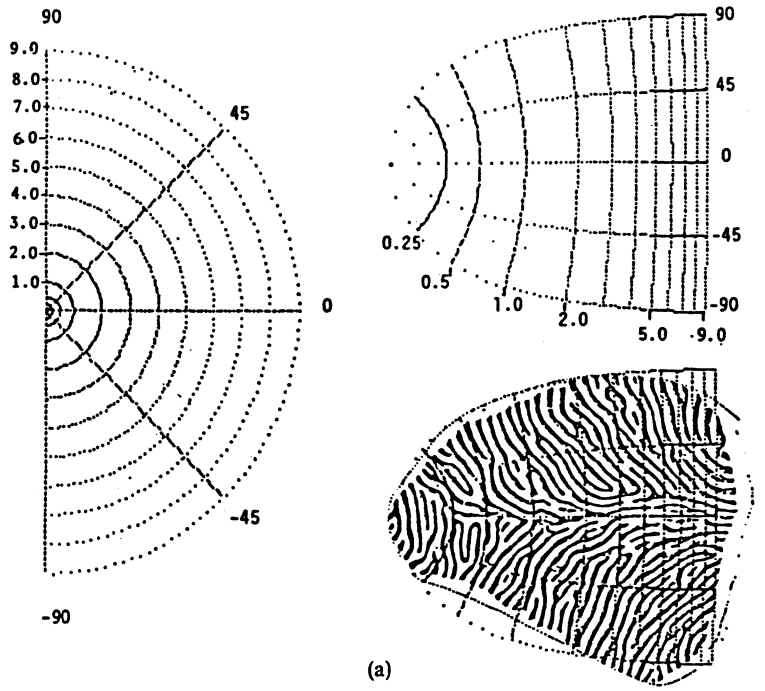

(a)

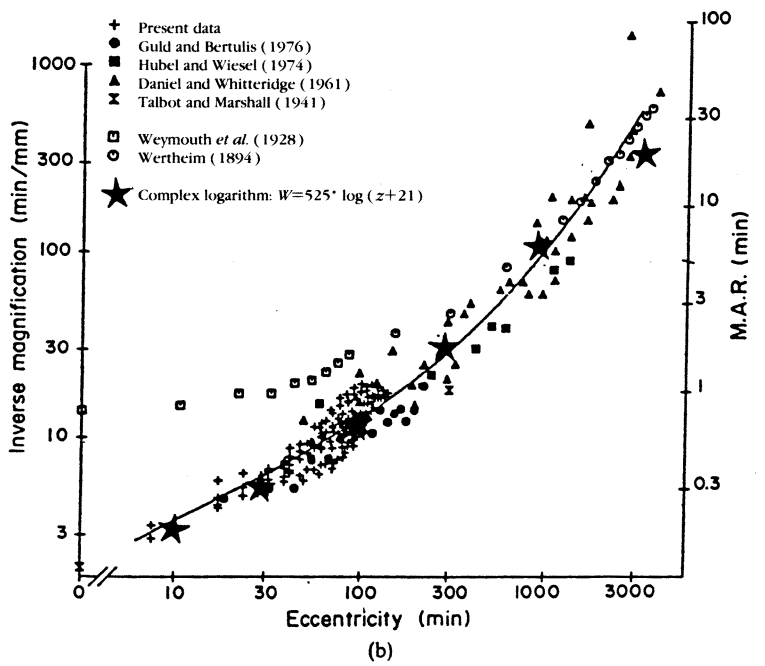

(b)

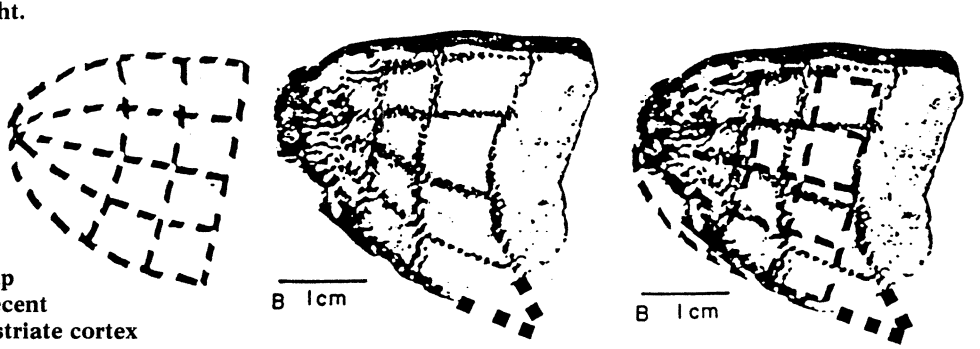

(c)

Figure 1.
At the top (a) is a representation of the visual field (or surface of the retina) on the left with a superposition of the anatomical data of Levay et al.[18] on the right. In the center (b) is a reprint of the magnification data of Dow et al.[6] together with other previous data. Superimposed over this fit (with large starts) is the estimate from the map function log (z+0.3). On the bottom (c) is a superposition of the map function log (z+0.3) (left), a recent deoxyglucose map of monkey striate cortex (center, Tootel et al.[10]), and a superposition of the theoretical and experimental maps (right).

Figure 2. This figure shows a single section (40 microns thick) of macaque striate cortex, prepared from a one-eyed monkey. The lack of input from one eye, over a period of some months, caused a depression in metabolic activity to the termination site of that eye.

The fundamental idea that emerges from the observations summarized above is that the primate brain is characterized (at least in its cortical structures) by an exquisite degree of spatial order on multiple spatial scales spanning the region from 1 mm^2 to roughly 1000 mm^2.

In the present article we focus on two areas of computer graphics and image processing applications that are critical to the understanding of cortical architecture. First we illustrate the technical application of computer graphics methods to brain reconstruction, flattening, and display of cortical surfaces. Then we show some examples of realistic simulation of the pattern of neural activity that occurs at the level of the medium scale (> 1 mm) architecture of primate striate cortex when various scenes in the world are viewed by the organism.

Differential geometry of the cortical surface and an optimal flattening algorithm

Much of the data on the functional architecture of visual cortex is acquired by painstaking recording with single microelectrodes, and from anatomical methods in which some form of "stain" is used to visualize the patterns as a whole. In recent years the anatomical methods have come to be of great importance. For example, it is possible to "stain" a pattern of metabolic activity linked to long-term (weeks, cytochrome oxidase) or fairly short-term (tens of minutes, 2 deoxyglucose) stimulation.

The 2 deoxyglucose (2DG) method is particularly powerful: It is possible to show an image to a primate and, using this technique,[10–12] produce an image of the associated neural activity on the surface of the brain. One of the principal limitations of the exploitation of the 2DG technique has been the technical problem of reconstructing and displaying the "images" that are buried in the convoluted cortex, and that are obtained in the form of serial sections. Because this technique is so powerful, it increases the need for development of computer-aided anatomical methods that would allow the computer graphic reconstruction and accurate representation, in both 3D and 2D form, of this data.

This problem can best be appreciated by viewing Figure 2, which shows a serial section of a monkey brain that has been stained, using cytochrome oxidase, to reveal the pattern of ocular dominance columns. This overall pattern is essentially an image, one that must be reconstructed and then displayed in an unfolded and flattened format. The act of flattening must not introduce unknown distortions of the tissue, since the metric relations of the image are important. For example, one might wish to measure angular relations between intersecting columnar systems, or topographic mapping data.

The problem might be symbolically phrased as follows: Take a photograph, crumple it up, slice the crumpled ball into hundreds of very thin sections, and then give the sections to someone who has the job of using computer graphics techniques to put the sections back together and then flatten the picture back into an unfolded representation, introducing minimal (and known) errors in the process. At the same time remember that it is a photograph, and not an abstract surface, that must be recovered.

This is a formidable problem of image processing, computer graphics, numerical mathematics, and neuroanatomical technique. The complete solution to it is a workable system of computer-aided anatomy. In the following section we describe one of the essential steps in the development of such a process: a characterization of the differential geometry of a typical cortical surface, and an algorithm for flattening this surface with minimal error.

Differential geometry of cortical surfaces

As outlined above, it is desired to flatten a curved surface with minimal error. A brief discussion of some ideas from differential geometry will illuminate this problem.

If a curved surface can be flattened into the plane with no error in the distances of points (the metric), then the mapping that affords this flattening is called an isometry. An example is a cylinder, whose surface may be isometrically mapped to the plane (unroll it). Many—actually, most—surfaces are not isometric to the plane. A sphere (or a part of a sphere) cannot be mapped into the plane with zero error. This is the so-called mapmaker's problem: Some compromise, reflected in the many different kinds of maps that exist for the earth, must be made.

The mathematical expression of the above discussion is based on the notions of mean and Gaussian curvature of a surface. At each point of the surface, one may fit circles to the point, and any two of its neighbors. These circles must lie in "normal sections"—a circle must lie in a plane containing the normal to the surface, and be defined by the chosen three points.[2] If one obtains all such circles at a point of a surface, there will be a maximum and minimum radius in this set (or they may all be equal). The average of the minimum and maximum radii is called the "mean" radius of curvature of the surface, and the (signed) square root of the product of the two radii is called the "Gaussian" radius of curvature.[2]

In terms of the previous two examples, a cylinder and a sphere, we can easily illustrate the concept of mean and Gaussian curvature. For the case of the cylinder of radius r, the maximum and minimum radii of curvature are r and 0. Thus, the mean and Gaussian radii of curvature are $r/2$ and 0, respectively. For the sphere, the maximum and minimum radii of curvature are r. Thus, the mean and Gaussian radii of curvature are $r/2$ and r. A general result is that if a surface is to be isometric to the plane, then its Gaussian curvature must be zero everywhere. Thus, the cylinder is isometric to the plane and the sphere is not. The cylinder can be perfectly flattened, while some

unavoidable error will be introduced in flattening a sphere. More generally, the mean and Gaussian curvature, at each point of a surface, provide a characterization of the surface.

We have begun our studies by measuring the mean and Gaussian curvature of the opercular surface of striate cortex. If the Gaussian curvature of the cortex is small, then it is possible to flatten it in a quasi-isometric way. Conversely, an understanding of the detailed curvature of this surface is necessary in order to understand the errors associated with flat representations.

We have developed anatomical methods, described in detail elsewhere,[1] that allow us to obtain accurate alignment of our serial sections with respect to the original, solid brain. These serial sections have been digitized via a CCD camera, and thresholding methods are used to obtain the outline of the outer surface of the brain. These outlines are then used to obtain a polyhedral model of the brain surface. Figure 3 shows a smooth-shaded (Gouraud) version of this polyhedral model of the opercular surface of the brain of a macaque monkey, and the underlying polyhedral model.

We have obtained the mean and Gaussian curvature of this surface by the method of fitting circles, in normal section, to each node of the polyhedral brain model, as described above. The mean and Gaussian curvature are illustrated in Figure 4. This is a pseudocolored, smooth-shaded polyhedral model, in which a "heat" scale represents the magnitude of mean and Gaussian curvature at each node of the polyhedral surface.

The typical radii of curvature of this brain surface range from less then 1 mm (in the region of the external calcarine sulcus) to a more typical value in the range of 1 to 1.5 cm. Over most of the surface, the Gaussian curvature is relatively constant: It behaves like a fairly small section of a sphere. This suggests that flattening cortex with relatively little error is possible. However, since the Gaussian curvature is not identically zero, we expected some difficulty in flattening this surface into a planar model of those regions (such as the sulci and the edges of the operculum) where our measurements indicated much larger than average amounts of Gaussian curvature. In particular, we expected larger than average errors in the region of the sulcus (for example, the external calcarine sulcus in Figures 3 and 4).

Two generic approaches to flattening a complex surface have occurred to us. First, one might try to physically simulate the motion of a surface moving under some system of forces. For example, the material of the brain could be modeled as an isotropic elastic substance that is moving under a constant pressure—we would "blow up" the surface, as in blowing up a folded balloon, and flatten the resultant spherical surface by conventional mapping methods. Secondly, one might formulate a variational problem in which some goodness-of-fit criterion was optimized. We have chosen the latter approach and have implemented algorithms that allow us to obtain optimal "near isometries" of surfaces such as the brain surface of Figure 3.

The first step is to formulate the variational problem. Since we seek optimal preservation of metric structure in the 3D and flattened models, we have chosen to maximize the goodness of fit of the "distance matrix" of the original 3D model and the flattened model of the brain. The distance matrix is defined as the matrix of all possible interpoint distances. Thus, in a polyhedral model of a surface, the distance between nodes i and j is called $d(i,j)$. Note that in the polyhedral model, distances must be defined as minimal geodesic distances, along paths embedded in the surface. This ensures that there will be a sensible match between straight line distances in the plane, which are minimal geodesic distances, and distances defined in this way on the polyhedron. It is a difficult computational problem to find minimal geodesic distances on arbitrary polyhedrons.

In the (unknown) flattened model, the same nodes i and j have an (unknown) distance between them, which we term $\tilde{d}$. The distance matrices d and $\tilde{d}$ are symmetric, are zero along their diagonals (i.e. lower triagonal matrices), and consist of

$$N\frac{(N\text{-}1)}{2}$$

distances for a model of N nodes.

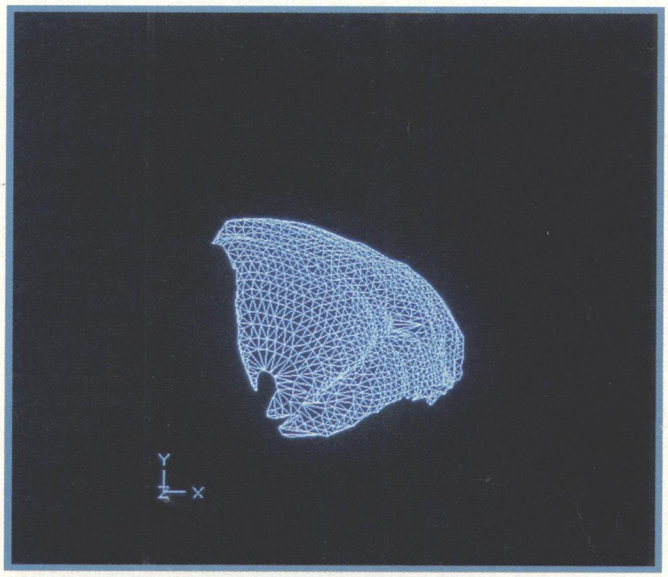

a

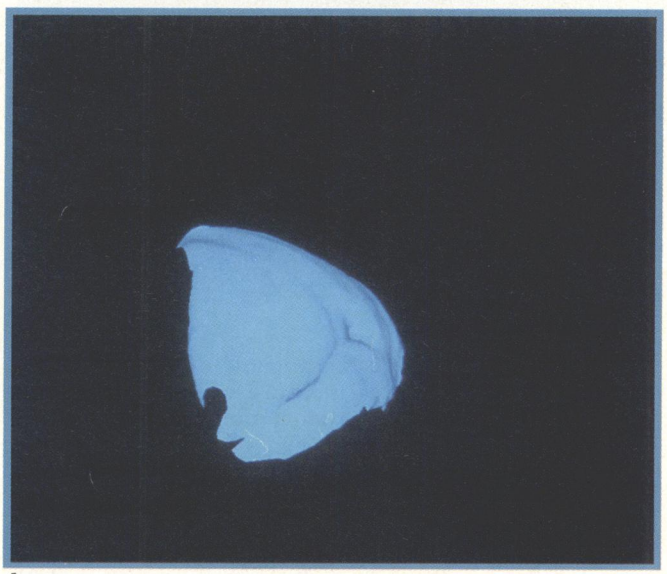

b

Figure 3. Several hundred of the sections represented in Figure 2 were carefully aligned by methods described in other work.[1] In (a) solids modeling techniques were used to construct a 3D polyhedral surface from these sections. In (b) this polyhedron was then shaded by the Gouraud algorithm to produce the shaded rendering.

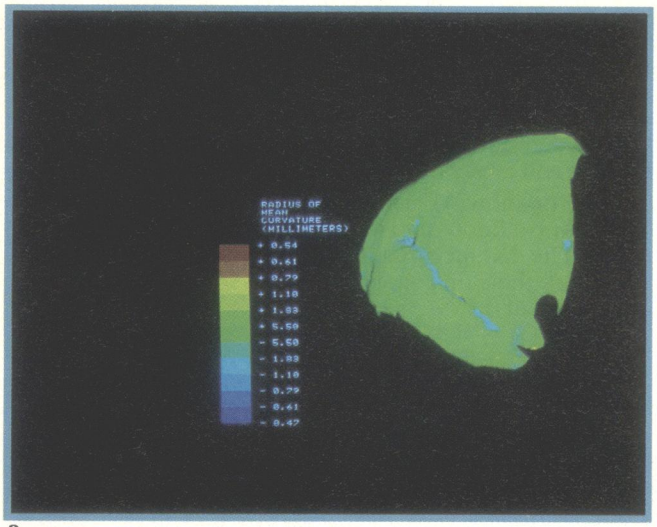

a

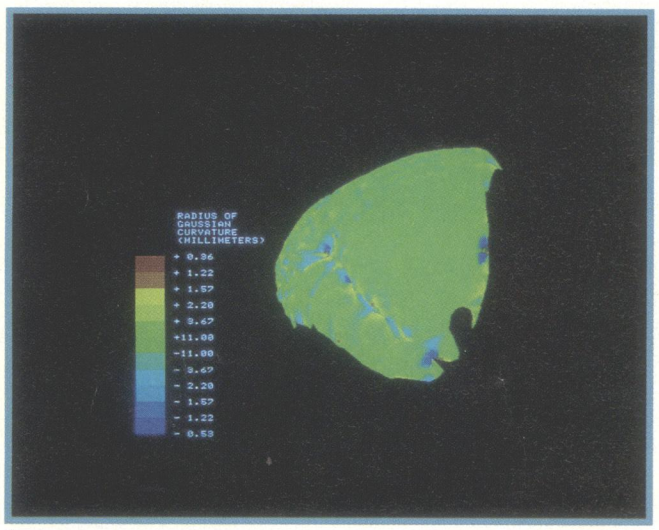

b

Figure 4. The opercular surface of Figure 3 is displayed (a) with an overlay of its mean and (b) Gaussian curvature illustrated by a "heat scale" technique. The mean and Gaussian curvature at each node of the polyhedral surface model have been measured, and a color indicating the magnitude has been smooth shaded into the surface.

The quantity L (the "Lagrangian" of this problem) represents a least-squares measure of fit between the metric structure of the original polyhedron and the planar model.

We define the goodness of fit of the two sets of distance matrices as follows:

$$L = \frac{1}{c}\sum_{i<j}^{i=N} \frac{(d_{ij} - \tilde{d}_{ij})^2}{d_{ij}} \qquad \textbf{(1.0)}$$

$$c = \sum_{i<j}^{i=N} d_{ij} \qquad \textbf{(1.1)}$$

$$\tilde{d}_{ij} = \sqrt{\sum_{k=1}^{k=2} (y_{ik} - y_{jk})^2} \qquad \textbf{(1.2)}$$

Minimizing the quantity L of Equation 1 may be performed by standard gradient descent algorithms.[13] We have used a quasi-Newton-Raphson method in which each iteration of the algorithm moves in the direction of the current gradient by an amount determined by the current second-order partial derivatives of the goodness of fit defined in Equation 1 above.

One serious difficulty in implementing this approach is deriving a means of measuring distances along an arbitrary polyhedral surface, a difficult problem that has only recently received attention. A similar problem arises in robotics motion planning, where the environment of the robot is modeled as a polyhedral space. Several approaches to the problem of calculating distances in polyhedral spaces have recently been described.[14] However, the thrust of these algorithms has been to calculate single paths of minimum length, given the initial and final points. Our problem is quite different, since we must calculate all (or many) of the possible distances.

We have implemented an algorithm to perform this distance calculation, which is described elsewhere,[15] and applied this algorithm to the brain data base shown in Figure 3 above. The basic polyhedral model consisted of approximately 1000 nodes. Since the variational algorithm is iterative, and since its complexity increases with the square of the number of nodes, it was of great importance to limit the number of elements in the distance matrix.

Initial runs in which only nearest-neighbor distances were used were not successful. The planar surface would have large folds in it, and an apparent lack of "rigidity" of the model allowed large local shears to develop. However, extending the allowed distances to a ring of at least second-nearest-neighbor nodes appeared to have added sufficient constraints to allow for the generation of good solutions to the flattening problem. In the examples shown, we have obtained a fairly good starting condition for the algorithm by crudely "stretching" contours and laying them down in the plane. This gives successful flattening with a second-nearest-neighbor distance measure.

In later work, with the same data, we have found that it is possible to use a random starting configuration and still achieve a good flattening, provided that a larger distance neighborhood is used. With the data shown in this article, neighborhoods of at least six to eight nodes about each node provide good results. The power of this algorithm is that by extending the neighborhood further out from each node, a good flattening is virtually guaranteed (although at a steeply rising cost in computer time).

Also, since obtaining a good starting configuration is itself a difficult problem (with complicated surfaces) that often requires substantial human interaction, a larger neighborhood—even though it costs more in terms of computer resources—is economical with respect to our own time. Finally, by starting from several different random starting configurations and comparing the end results, one can gain confidence that the solution is robust and correct. In our initial testing we have found that different random starting configurations converge to virtually identical final states.

Since our algorithm for determining geodesic distances[15] is capable of extension to arbitrarily large neighborhoods, and since we are getting excellent results with rather small neighborhoods, we feel that this method is likely to succeed with even the most difficult cortical surfaces one is likely to encounter in the vertebrate brain.

Figure 5 below shows an example of the flattened opercular surface of striate cortex, based on a distance matrix that includes all distances in a ring around each node in which at least second-nearest neighbors are included in the variational calculation.

Figure 6 shows a wire frame model of the flattened surface, and a map of the error introduced in the flattening. The error is defined to be the signed difference in the length of each node in the original (3D) and flattened (2D) model. As seen, the typical error is on the order of 1 percent, although localized regions of higher curvature (the lateral calcarine sulcus, the curved edges of the operculum) have errors that are in the range of 3 to 5 percent, with a maximum error in a few spots of about 15 percent.

The small errors obtained, together with an agreement of the location of these errors and regions of maximum mean and Gaussian curvature, support the accuracy of this flattening procedure. A further check is shown in

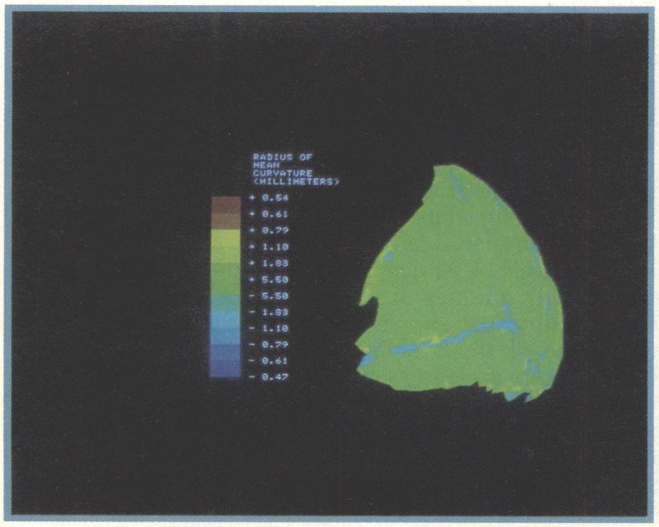

a

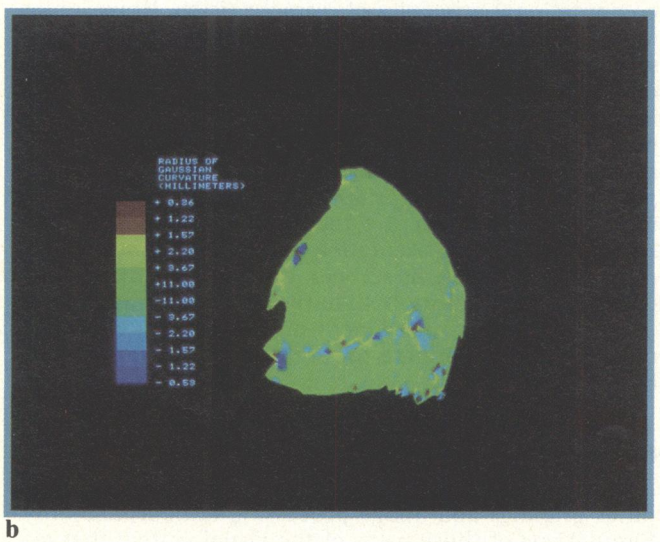

b

Figure 5. This figure displays (a) the same mean and (b) Gaussian curvatures of Figure 4, now overlayed over a flattened version of the surface. The flattening has been performed by the variational algorithm described in the text.

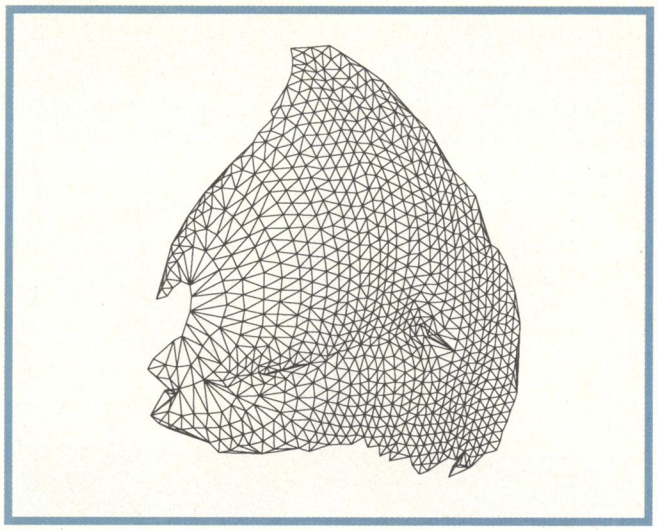

a

b

Figure 6. In (a) the wire frame model is the flattened operculum in polygonal format. In (b) a color-coded map of the errors introduced by the flattening algorithm is then overlayed on the flattened model.

Figure 7, which shows a superposition of our digital flattening over two specimens of monkey striate cortex operculum that have been flattened by careful dissection and pressing unfixed cortical tissue between glass slides. The approximate agreement in shape between the digitally and physically flattened cortical samples, together with the generally small errors in the digital flattening process, gives us confidence that this algorithm is performing correctly.

The work illustrated here is merely a first step in the development of a general set of tools for performing accurate reconstructions and measurements of neuroanatomical surfaces. Our motivation in developing these methods is for exploring the dozen or so areas of visual cortex now known to exist in the primate neocortex. With the exception of striate cortex, relatively little about these other areas has been detailed. However, striate cortex is well understood at the present time, at least with respect to the topographic map of the visual field that it contains

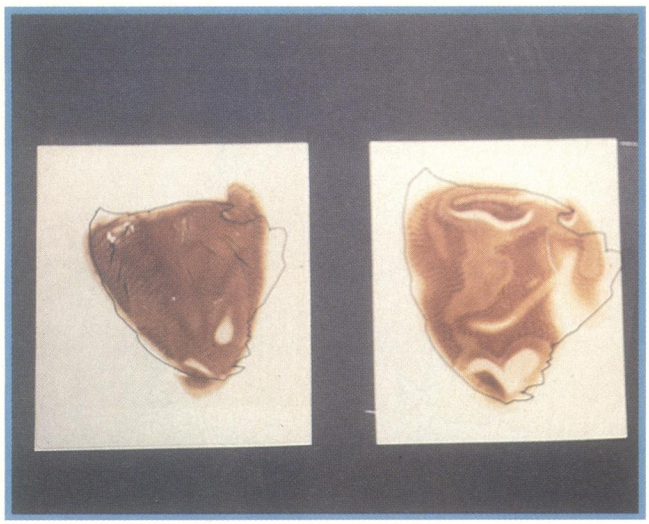

Figure 7. In this figure we have overlayed the flattened cortical specimen over two different samples of physically flattened operculum. The agreement between the digital and physically flattened material is good, especially considering that different animals were the source of each specimen, and that the physical flattening in particular is subject to many uncontrolled variables.

(e.g. Figure 1). In the next section of this article we demonstrate computer graphic simulations of the topographic map structure of striate cortex by using real photographic images, digitized to approximately the accuracy of the human visual system as they would appear on the surface of the striate cortex.

Computer graphics simulations of visual scenes mapped to the surface of striate cortex

Roughly 10 years ago, a map function of the form log $(z+a)$ was proposed as a functional form for primate striate cortex.[4,16] In this equation a is a small constant that recent measurement suggests is in the range of 0.3 to 0.7 degrees[5,6] and z is a complex variable. The use of complex variables is a great simplification, since it allows a one-parameter fit (based on the parameter a) to the entire 2D structure of the cortical map. The complex logarithmic mapping is a conformal mapping: It is locally isotropic and preserves (local) angles. If it can be shown experimentally that a given visual map is *locally* isotropic, then the map function for this area is conformal. Conformal maps, in general, have interesting computational properties for modeling cortical architectures, as well as potential applications in computational vision.[4,17]

The precise details of the striate cortex map are still controversial, which is one of the reasons we are developing the methods illustrated in the first part of this paper. Several authors have recently claimed to find small areas in which local isotropy may not hold.[5,10] Nevertheless, these same authors agree that the complex log mapping is a good approximation to the topographic structure of primary visual cortex.[7] In probably the most accurate study to date, based on extensive study of foveal cortex in awake monkeys, Dow et al.[6] have explicitly confirmed the map function log $(z + 0.3)$.

In Figures 8 and 9 we have used this map function to simulate the spatial structure of an image as it would appear at the surface of primate striate cortex. The input image was constructed using a mosaic technique and a CCD camera. The resolution of the Fairchild CCD camera is 380 × 488 pixels. The CCD sensor was mounted on a micromanipulator and moved accurately (with a resolution of about 10 microns) to construct the 1600 × 1580 image. The examples of images included here range from a field of view of 3 degrees to 50 degrees. For the 50-degree field, our sampling is on the order of 3 minutes of arc. (This is close to typical values for human visual acuity of about 1 minute of arc; for the smaller fields, we are sampling far beyond human acuity limits.)

A simulation of reading a newspaper, at conventional reading distance of 22 cm, is shown in Figure 8. Note that the strongly space-variant nature of the human visual system makes it difficult to resolve more than a few letters at a time. Computer animation of a reading sequence based on this text has recently been demonstrated.[8]

Also shown in Figure 8 is a simulated scanning of a face. The scan points are marked by small crosses in Figure 8. The scanning of the face and the scanning of the newspaper, in their cortical versions, represent a fairly realistic simulation of the play of neural activity across the surface of primary visual cortex associated with scanning these images.

An outdoor scene is shown in Figure 9. The original scene was photographed on high-resolution film (Kodak TP, Technidol), and a high-resolution mosaic (1600 × 1580) was prepared as discussed above. For a simulated viewing angle of 50 degrees of field the pixel size corresponds to 2 minutes of arc, still in the range of human visual acuity. Also shown in Figure 9 is a "retinal" view of the scene of the building. The air conditioner at the fixation point is clearly seen, with the typical rapid fall-off in detail caused by the space-variant nature of the human visual system. It is remarkable that individual bricks are clearly visible in the center of several of the cortical scans, while at the far peripheral end most of the building structure is collapsed into a comparable area of cortex.

We are still at an early stage of understanding of the computational principles of primate vision. However, as these simulations indicate, the primate visual system is strongly space variant and thus represents a very different set of problems from those of conventional, space-invariant machine vision systems. In previous work[17] it has been argued that the anatomy of the primate visual system represents a set of novel architectures for image processing: Specific algorithms that are contingent on the topographic map structure, the ocular dominance column structure, and the orientation column structure of primate striate cortex have been outlined. Further development of these ideas, both in the context of natural and machine vision, is contingent on our further ability to measure, and to simulate, the architectures of the primate brain.

Summary

We have demonstrated several applications of computer graphics and image processing in neuroanatomy. Simulations of those parts of the visual system that are reasonably well understood may provide some insight in to the nature of visual computation. Also, the data upon which this knowledge is based may itself benefit from the ability to perform neuroanatomical studies with the use of computer graphics methods. The algorithm for quasi-

a

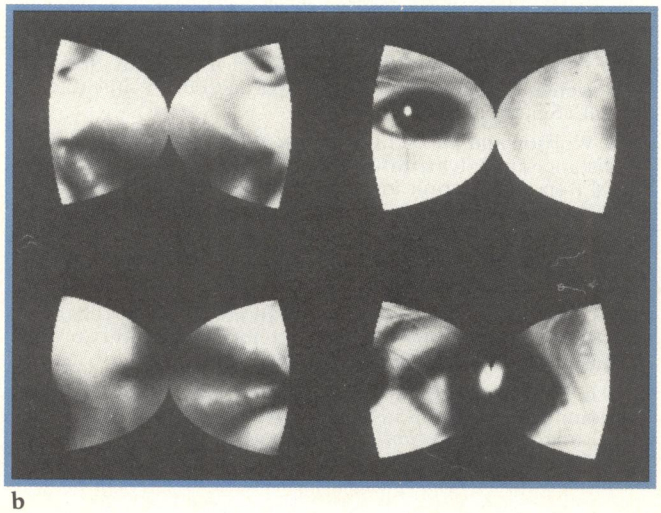

b

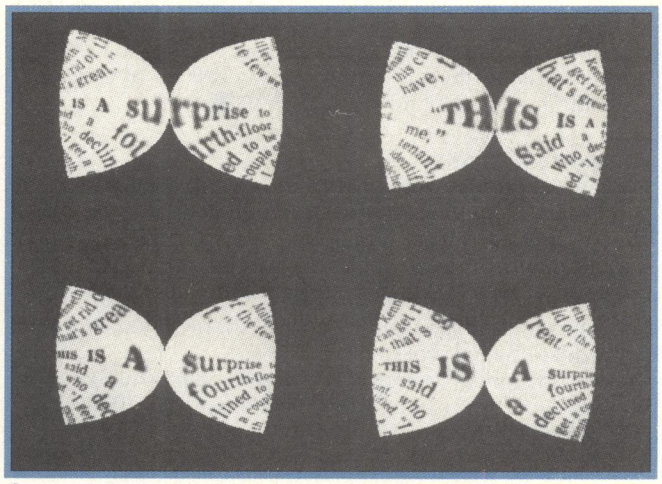

c

Figure 8. In (a), the reproduction of a face, four "fixation" points are indicated by small crosses: one in the center of the left eye, one at the right edge of the left eye, one on the upper lip and one on the lower lip. In (b) the cortical map for these fixation points is simulated, showing about 1.5 degrees on either side of them. The map function log $(z+0.3)$ is used. This figure can be understood in the following manner: If it were possible to image the surface of the cortex so that at each instant the image gave a measure of the firing density of cellular activity, then as the eyes scanned the scene in 8a, as described, the cortical "image" would be similar to that shown in the center of the figure. In (c) a similar simulation of reading newspaper text is made. The reading distance is 22 cm, and about 1.5 degrees on either side of the fixation points are shown. The text reads, "This is a surprise."

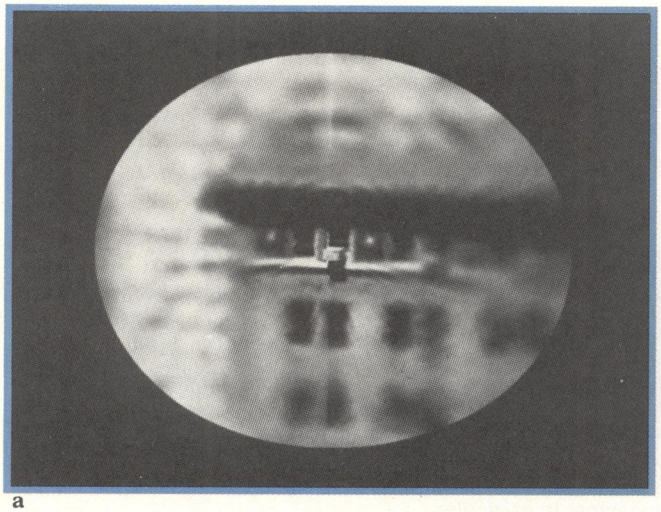

a

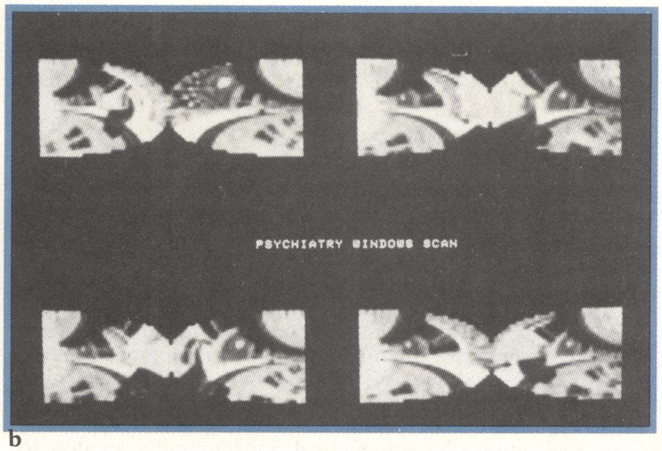

b

Figure 9. This outdoor scene for a 50-degree field of view includes the psychiatry building at NYU Medical Center. First this scene is shown with (a) a "fall-off" in visual resolution caused by the space-variant nature of the map function log $(z+0.3)$. Thus, the original high-resolution scene was mapped via log $(z+0.3)$ and then back-mapped to the "retina" with the inverse mapping function (the complex exponential). Then in (b) four log-mapped views of the same scene are shown. Note that individual bricks are clearly visible in the central foveal regions, and that toward the periphery the entire size of the building has been collapsed to roughly the size of the windows in the central representation. The distance of viewing for this 50-degree field was about one-quarter mile.

isometric flattening of complicated surfaces, which we have described and illustrated in this article, is a necessary first step in the development of a full set of tools for the field of computer-aided anatomy. ■

Acknowledgments

We thank Estarose Wolfson for many discussions, and for implementing the polyhedral distance algorithm. Thanks also to Wesley Kaplow, Alan Shaw, Nelson Gonzalez, William Light, Keith Lorris, Hedly Rainie, and Barbara Miller for their contributions to software development in this project. We also thank Amar Munsiff for his histological work.

Research for this article was supported by the Systems Development Foundation, AFOSR F49620-83-C0108, and AFOSR 85-0341.

References

1. B. Merker and E.L. Schwartz, "Computer-Aided Anatomy: Reconstruction and Characterization of the Opercular Surface of Macaque Striate Cortex," *Investigative Opthalmology Supplement (AVRO)*, Vol. 26, 1985, p.164.
2. M. do Carmo, *Differential Geometry of Curves of Surfaces*, John Wiley and Sons, New York, 1975.
3. D.H. Hubel and T.N. Wiesel, "Sequence Regularity and Geometry of Orientation Columns in Monkey Striate Cortex," *J. Comparative Neurology*, Vol. 158, 1974, pp.267-293.
4. E.L. Schwartz, "Spatial Mapping in the Primate Sensory System: Analytic Structure and Relevance to Perception," *Biological Cybernetics*, Vol. 25, 1977, pp.181-194.
5. D.C. Van Essen, W.T. Newsome, and J.H.R. Maunsell, "The Visual Representation in Striate Cortex of the Macaque Monkey: Assymetries, Anisotropies, and Individual Variability," *Vision Research*, Vol. 24, 1984, pp.429-448.
6. B. Dow, R.G. Vautin, and R. Bauer, "The Mapping of Visual Space onto Foveal Striate Cortex in the Macaque Monkey," *J. Neuroscience*, Vol. 5, 1985, pp.890-902.
7. R. Tootel, M.S. Silverman, E. Switkes, and R. DeValois, "Deoxyglucose Retinotopic Maps and the Complex Log Model in Macaque Striate Cortex," *Science*, Vol. 227, 1985, p.1066.
8. E.L. Schwartz, "Image Processing Simulations of the Functional Architecture of Macaque Striate Cortex," *Investigative Opthalmology Supplement (AVRO)*, Vol. 26, 1985, p.164.
9. M. Livingstone and D.H. Hubel, "Anatomy and Physiology of a Color System in the Primate Visual Cortex," *J. Neuroscience*, Vol. 4, 1984, pp.309-356.
10. R. Tootel, M.S. Silverman, E. Switkes, and R. DeVois, "Deoxyglucose Analysis of Retinotopic Organization in Primate Striate Cortex," *Science*, Vol. 218, 1982, pp.902-904.
11. E.L. Schwartz, D.R. Christman, and A.P. Wolf, "An Application of PETT Scanning to the Observation of Human Visual Cortex Topographic Mapping," *Neuro. Soc. Abstracts*, Vol. 7, 1981, p.351.
12. E.L. Schwartz, D.R. Christman, and A.P. Wolf, "Human Primary Visual Cortex Topography Imaged Via Positron Tomography," *Brain Research*, Vol. 294, 1984, pp.225-230.
13. J.W. Sammon, "A Nonlinear Mapping for Data Structure Analysis," *IEEE Trans. Computers*, C-18, 1969, pp.401-408.
14. M. Sharir, "Distance Calculations in Polygonal Spaces," Robotics Research Technical Reports, Courant Institute of Math Sciences, 1985.
15. E. Wolfson and E.L. Schwartz, "An Algorithm for Calculating Distances in Polyhedral Spaces," Robotics Research Technical Reports, Courant Institute of Mathematical Sciences (in preparation).
16. E.L. Schwartz, "Analytic Structure of the Retinotopic Mapping of Striate Cortex and Relevance to Perception," *Neuroscience Abstracts*, Vol. 6, 1976, p.1636.
17. E.L. Schwartz, "Anatomical and Physiological Correlates of Visual Computation from Striate to Infro-Temporal Cortex," *IEEE SMC*, Vol. 14, 1984, pp.257-269.
18. S.D. Levay, D.H. Hubel, and T.N. Wiesel, "The Pattern Ocular Dominance Columns in Macaque Visual Cortex Revealed by a Reduced Silver Stain," *J. Comparative Neurology*, Vol. 159, 1975, pp.559-576.

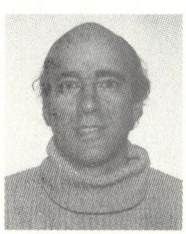

Eric L. Schwartz is associate professor at the Brain Research Laboratory of the NYU Medical Center, chief of the Human Visual Studies Laboratory at Nathan Kline Research Institute, and a visiting member of the faculty at the NYU Courant Institute of Mathematical Sciences. His current research interests are the anatomy and physiology of primate visual systems, computational vision and robotics, and computer and mathematical simulation of the nervous sytem. A major theme of this research is the application of mathematical and computer models to describe the various architectures that have been observed experimentally in primate visual systems, and to infer the possible computational significance of these architectures for both machine and biological visual computation.

Schwartz received an AB in physics and chemistry (1967) and MA, MPhil, and PhD in high-energy physics (1973) from Columbia University.

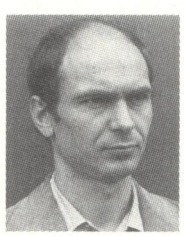

Bjorn Merker is research assistant professor at the Brain Research Laboratory of the NYU Medical Center. Prior to his current work on the primate visual system, he worked on behavioral consequences of brain lesions in hamsters, neuroanatomical staining and lesioning methods, and the control of eye movements in the cat. His interests include the functional significance of spatial and geometric aspects of brain structures in general and the computational significance of topographic mappings in particular.

Merker received an AB in psychology from Queens College of the City University of New York in 1975, and a PhD in psychology and brain science from the Massachusetts Institute of Technology in 1980. He was born in 1943 and is a Swedish citizen.

The authors can be contacted at the Brain Research Laboratory, NYU Medical Center, 550 First Ave., New York, NY 10016; (212) 340-6299.